

EFFICIENCY OF NOISE REDUCTION BY A ROAD SPEED BUMP

Rufin MAKAREWICZ, Piotr KOKOWSKI

Adam Mickiewicz University
Institute of Acoustics
Umultowska 85, 61-614 Poznań, Poland
e-mail: makaaku@amu.edu.pl, pikoko@spl.ia.amu.edu.pl

(received January 31, 2007; accepted May 28, 2007)

The vehicle noise from a road with a bump consists of the deceleration noise, bump noise, and acceleration noise. The bump is modeled by the Dirac delta function. The linear density of sound energy (in Joules per meter) is used for the calculation of sound energies, e_c and e , emitted by a vehicle on a road without- and with a bump, respectively. The ratio $\eta = (e_c - e)/e$ defines the efficiency of noise reduction by a speed bump. To determine η , four measurements of the sound exposure level have to be done. The example of such measurements and calculation of η is given.

Keywords: road traffic noise, noise reduction, speed bump.

1. Introduction

During the cruise mode of motion at a steady speed, the sound power of a vehicle is constant. While the vehicle approaches the bump, the sound power decreases. Then, due to the wheel impact on the bump and vehicle body vibration, the bump noise appears. It is characterized by a spike-like change of the sound power. Later, during departure, the sound power increases and finally achieves again the cruise sound power. The question is, how much the speed bump reduces or increases the total sound energy.

This problem was addressed in Ref. [1] under rather flimsy assumption: the bump noise can be neglected. In the present paper it is taken into account. The use of the linear density of sound energy (expressed in Joules per meter) differentiates this study from the others, which consider the stop-and-go traffic noise [2–11].

2. Linear density of sound energy

A road vehicle is modeled by a nondirectional point source (see ref. [12]) with the A -weighted sound power W_A . Above an acoustically hard surface, a few tens of meters from the road (at the first row of buildings), the geometrical spreading predominates the

ground effect and the noise reflection beneath the vehicle yields a virtual change in the A -weighted sound power, $W_A \rightarrow \beta W_A$.

Suppose the noise source S moves along the x -axis. Assuming $H \gg h$ (Fig. 1) we introduce the perpendicular distance between the source track and the receiver M ,

$$d \approx \sqrt{D^2 + H^2}, \tag{1}$$

and obtain the instantaneous distance between $S(x, 0)$ and $M(X, d)$ (Fig. 2),

$$r = \sqrt{d^2 + (x - X)^2}. \tag{2}$$

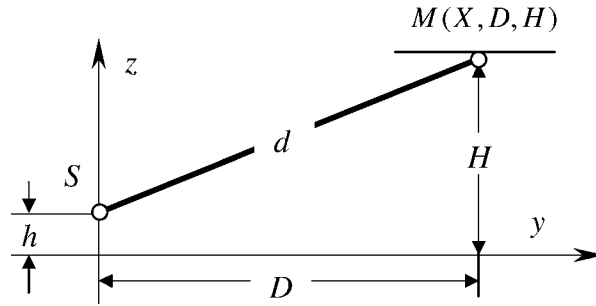


Fig. 1. The perpendicular distance d (Eq. (1)) between the track of the source S and the microphone M .

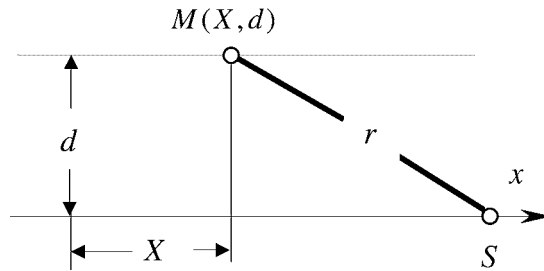


Fig. 2. Location of the microphone M , determined by the perpendicular distance d and the longitudinal distance X , with the vehicle S moving at the velocity V along the x -axis.

Hence, the A -weighted squared sound pressure of the noise produced by the vehicle equals

$$p_A^2(r) \approx \frac{\beta W_A \rho c}{4\pi r^2}, \tag{3}$$

where ρc is the characteristic impedance of air. In practice, traffic noise propagation is affected by buildings reflection, air absorption, refraction, and scattering by atmospheric turbulence [13]. Consequently, the dependence of p_A^2 upon the distance r becomes quite complex. However, within tens of meters from the road axis, the most important phenomena are geometrical spreading and reflection from the road surface, so Eq. (3) seems to be relevant.

When the source S moves at a varying velocity $V(x)$, the time increment $dt = dx/V(x)$ brings about a change in the sound exposure (Fig. 3) [1],

$$dE = \frac{p_A^2(x)}{V(x)} dx. \tag{4}$$

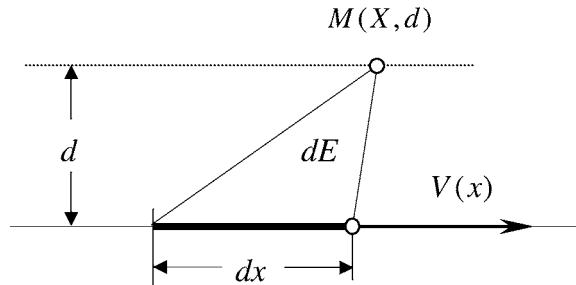


Fig. 3. Increment of the sound exposure dE (Eq. (4)) due to the infinitesimal displacement of the source dx .

Equations (3) and (4) imply the sound exposure of noise from the road segment (x_1, x_2) (Fig. 4),

$$E(x_1, x_2) = \frac{\rho c}{4\pi} \int_{x_1}^{x_2} \frac{S(x)}{r^2(x)} dx, \tag{5}$$

where

$$S(x) = \frac{\beta W_A(x)}{V(x)}, \tag{6}$$

is the linear density of sound energy, expressed in Joules per meter [1, 14–16]. The function $S(x)$ characterizes the sound energy which is shed by a source moving along its track i.e. the x -axis.

The cruise mode of motion at a steady speed V_c and a constant A -weighted sound power $(\beta W_A)_c$, is described by the uniform radiation of energy along the x -axis. In such a case the linear density of the sound energy is (Eq. (6)),

$$S(x) = S_c. \tag{7}$$

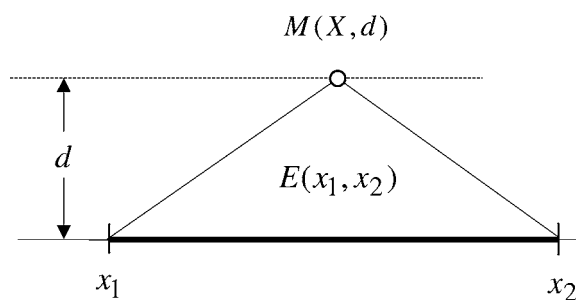


Fig. 4. Sound exposure $E(x_1, x_2)$ (Eq. (5)) of noise coming from the road segment (x_1, x_2) .

The road with a bump has two cruise segments: $-\infty < x < -l_1$ and $+l_2 < x < +\infty$ (Fig. 5).

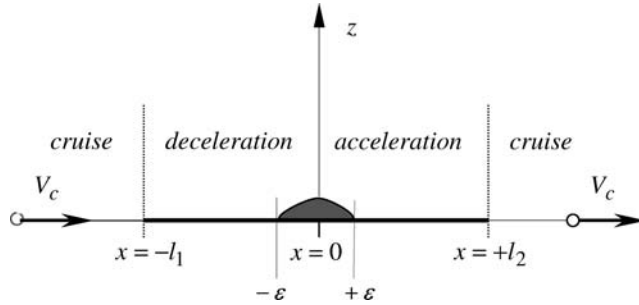


Fig. 5. A road consisting of the cruise parts $(-\infty, -l_1)$, $(+l_2, +\infty)$, deceleration and acceleration parts $(-l_1, -\epsilon; +\epsilon, +l_2)$, with the very narrow bump $(-\epsilon, +\epsilon)$ between them.

During deceleration, both the A -weighted sound power $\beta W_A(x)$ and the velocity $V(x)$ decrease along the road segment $-l_1 < x < -\epsilon$, where $\epsilon \rightarrow 0$ denotes half width of the bump (Fig. 5). It is assumed that the corresponding density of the sound energy declines parabolically to zero (Fig. 6),

$$S_1(x) = S_c \cdot \left[-\frac{x}{l_1} \right]^2, \tag{8}$$

where l_1 is the unknown acoustical length of deceleration (see Sec. 4.1). The above relationship is not yet empirically proved. At the start of deceleration ($x = -l_1$), the linear density of the sound energy meets the condition, $S_1 = S_c$. At the end of deceleration, when the vehicle approaches the bump ($x \rightarrow 0$), the power unit noise and tyre/road noise tend to zero, thus one can write, $S_1 \rightarrow 0$ (Fig. 6, Eq. (8)).

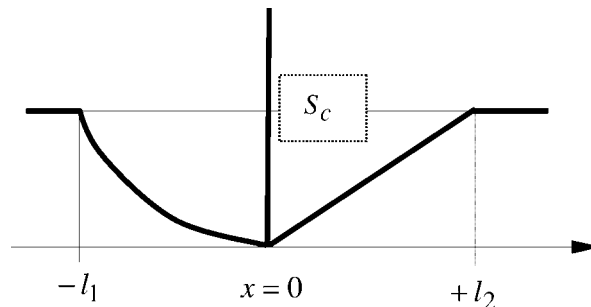


Fig. 6. Linear density of sound energy $S(x)$ for a road segment with a bump (Eqs. (7)–(9), (11)).

The bump noise is emitted from the road segment, $-\epsilon < x < +\epsilon$ (Fig. 5). It comes from the vehicle body vibrations, produced by the wheels impact on the bump. The linear density of the sound energy of the spike like bump noise is modeled by (Fig. 6),

$$S_b = l_b S_c \delta(x), \tag{9}$$

where l_b is the bump noise coefficient (see Sec. 4.2), and S_c is the linear density of sound energy for the cruise mode of vehicle motion (Eq. (7)). For any function $F(x)$ continuous at $x = 0$, the Dirac delta function $\delta(x)$ meets the condition [17],

$$\lim_{\varepsilon \rightarrow 0} \int_{-\varepsilon}^{+\varepsilon} F(x) \delta(x) = F(0). \quad (10)$$

During acceleration, both $\beta W_A(x)$ and $V(x)$ increase along the road segment, $+\varepsilon < x < l_2$ where $\varepsilon \rightarrow 0$ (Fig. 5) and the following dependence of the linear density of sound energy on the distance x is assumed,

$$S_2(x) = S_c \cdot \left[+\frac{x}{l_2} \right], \quad (11)$$

where l_2 is the unknown acoustical length of acceleration (see Sec. 4.3). Similar to Eq. (8), the above relationship is not empirically founded. At the start of acceleration ($x \rightarrow 0$) and at the end of acceleration ($x = l_2$) one gets $S_2 \rightarrow 0$ and $S_2 = S_c$, respectively (Fig. 6).

3. Sound energy

The efficiency of noise reduction due to a road bump is defined by:

$$\eta = \frac{e_c - e}{e_c}, \quad (12)$$

where e_c is the total noise energy emitted from the road segment of the length $l_1 + l_2$ without a bump, and e is the total sound energy emitted from the same road segment with a bump. Note, that bump efficiency expressed in terms of energy is independent on both propagation conditions as well as receiver's position, M (Figs. 1, 2).

When $e_c \rightarrow e$ the above definition yields the vanishing efficiency: $\eta \rightarrow 0$. Because $S(x)$ denotes the amount of sound energy emitted from the track of a unit length (Eq. (6)), thus the total sound energy from the road segment $l_1 + l_2$ with a bump is,

$$e = \int_{-l_1}^{-\varepsilon} S_1(x) dx + \int_{-\varepsilon}^{+\varepsilon} S_b(x) dx + \int_{+\varepsilon}^{+l_2} S_2(x) dx. \quad (13)$$

Equations (8)–(11), (13) yield the total sound energy,

$$e = S_c \left[\frac{1}{3}l_1 + l_b + \frac{1}{2}l_2 \right]. \quad (14)$$

Without a bump, there is a uniform distribution of the sound energy along the road segment $l_1 + l_2$, and $S(x) = S_c$ for $-l_1 < x < +l_2$. Consequently, the corresponding value of the total sound energy equals,

$$e_c = S_c \cdot [l_1 + l_2], \quad (15)$$

and the efficiency of noise reduction due to a bump can be calculated from (Eqs. (12), (14), (15)),

$$\eta = \frac{2l_1 + 6l_b + 3l_2}{6(l_1 + l_2)}. \quad (16)$$

To determine η , the acoustical lengths of deceleration and acceleration (l_1, l_2), as well the bump noise coefficient (l_b) are needed. In the next section it will be shown how to determine all of them from the measurements of the sound exposure level L_{AE} .

4. Sound exposure level

The directly measurable sound exposure level is defined by:

$$L_{AE} = 10 \log \left\{ \frac{E}{p_0^2 \cdot t_0} \right\}, \quad (17)$$

where the reference sound pressure $p_0 = 20 \mu\text{Pa}$, the unit time $t_0 = 1 \text{ s}$, and the sound exposure E is defined by Eq. (5). In this study the measurements of L_{AE} for light vehicles were performed with the sound level meters SVAN 945, equipped with a GRASS 49AN microphones, located at the height $H = 1.2 \text{ m}$ above the concrete pavement, at the horizontal distance $D = 7.5 \text{ m}$ from the vehicle track (Fig. 1). Using Eq. (1) we got the perpendicular distance between the road axis and the microphone: $d = 7.6 \text{ m}$. For each vehicle, 4 measurements of L_{AE} were made at a varying longitudinal distance X and at a constant perpendicular distance d , namely: $L_{AE}^{(a)}(-X_1)$ and $L_{AE}^{(a)}(0)$ for the approach noise, $L_{AE}^{(b)}(0)$ for the bump noise, and finally, $L_{AE}^{(d)}(0)$ for the departure noise. The weather was windless and sunny.

4.1. Approach noise

The approach noise is emitted by the vehicle during its travel from $x = -\infty$ to the bump, $x = -\varepsilon$ (Fig. 5). It consists of the cruise noise ($-\infty, -l_1$) and deceleration noise ($-l_1, -\varepsilon$), where $\varepsilon \rightarrow 0$ (Fig. 6). For the microphone M at the longitudinal distance X from the bump ($x = 0$), the corresponding sound exposure level is $L_{AE}^{(a)}(X, l_1)$ (Eq. (17)), where the sound exposure of the approach noise has two components,

$$E_a(X, l_1) = E_{c1}(-\infty, -l_1) + E_1(-l_1, -\varepsilon), \quad (18)$$

where $\varepsilon \rightarrow 0$. The cruise noise is characterized by (Eqs. (2), (5), (7)),

$$E_{c1} = \frac{\rho c}{4\pi} S_c \int_{-\infty}^{-l_1} \frac{dx}{(x - X)^2 + d^2}, \quad (19)$$

and the deceleration noise by (Eqs. (2), (5)),

$$E_1 = \frac{\rho c}{4\pi} \int_{-l_1}^{-\varepsilon} \frac{S_1(x) dx}{(x - X)^2 + d^2}, \quad (20)$$

where $\varepsilon \rightarrow 0$ and the linear density of sound energy $S_1(x)$ is defined by Eq. (8). After some calculations we arrive at (Eqs. (18)–(20)),

$$E_a(X, l_1) = \frac{\rho c S_c}{4\pi d} F_a(X, l_1), \quad (21)$$

where

$$F_a(X, l_1) = \frac{\pi}{2} - \tan^{-1}\left(\frac{l_1 + X}{d}\right) + \frac{X^2 - d^2}{l_1^2} \left[\tan^{-1}\left(\frac{l_1 + X}{d}\right) - \tan^{-1}\left(\frac{X}{d}\right) \right] + \frac{d}{l_1} - \frac{Xd}{l_1^2} \ln \frac{(l_1 + X)^2 + d^2}{X^2 + d^2}. \quad (22)$$

The sound exposure level of the approach noise is (Eqs. (17), (21)),

$$L_{AE}^{(a)}(X) = L_s + 10 \log \left\{ \frac{d_0}{4\pi d} F_a(X, l_1) \right\}, \quad d_0 = 1 \text{ m}, \quad (23)$$

where

$$L_s = 10 \log \left\{ \frac{S_c}{S_0} \right\}, \quad S_0 = 10^{-12} \text{ [J/m]}, \quad (24)$$

defines the level of the linear density of sound energy for the cruise segment of the source approach, $x < -l_1$ (Figs. 5, 6). The perpendicular distance from the track, d , and the longitudinal distance from the bump, X , determine the microphone location (Fig. 2). The level of the linear density of sound energy, L_s , and the acoustical length of deceleration, l_1 , are free parameters of the model. To estimate their values, two simultaneous measurements of the sound exposure level $L_{AE}^{(a)}(X)$ of the approach noise must be performed (Fig. 7): the first at the longitudinal distance $X = -X_1$ (left from the bump) and the second at the longitudinal distance $X = 0$ (opposite the bump middle). Making use of Eq. (22) one gets two equations with two unknowns, L_s and l_1 ,

$$L_{AE}^{(a)}(-X_1) = L_s + 10 \log \left\{ \frac{d_0}{4\pi d} F_a(-X_1, l_1) \right\}, \quad (25)$$

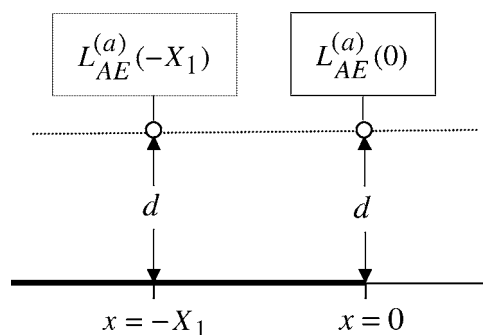


Fig. 7. Microphones location at two simultaneous measurements of approach noise.

and

$$L_{\text{AE}}^{(a)}(0) = L_s + 10 \log \left\{ \frac{d_0}{4\pi d} F_a(0, l_1) \right\}. \quad (26)$$

Because $L_{\text{AE}}^{(a)}(-X_1)$ and $L_{\text{AE}}^{(a)}(0)$ represents the measurement output, Eqs. (25) and (26) enable determination of the acoustical length of deceleration, l_1 ,

$$\frac{F_a(-X_1, l_1)}{F_a(0, l_1)} = 10^{0.1[L_{\text{AE}}^{(a)}(-X_1) - L_{\text{AE}}^{(a)}(0)]}, \quad (27)$$

where the explicit forms of $F_a(-X_1, l_1)$ and $F_a(0, l_1)$ are determined by Eq. (22).

Consequently, using the calculated value of l_1 and Eq. (26), one can find the second parameter of the model, namely L_s .

Example 1

The results of 71 measurements of $L_{\text{AE}}^{(a)}(-X_1)$ and $L_{\text{AE}}^{(a)}(0)$ are shown in Fig. 8. Two microphones were located at $(X_1 = 20 \text{ m}, d = 7.6 \text{ m})$ and $(X_1 = 0, d = 7.6 \text{ m})$. The average values of the sound exposure levels are: $L_{\text{AE}}^{(a)}(-X_1) = 70.5 \text{ dB}$ and $L_{\text{AE}}^{(a)}(0) = 65.6 \text{ dB}$. With the perpendicular distance $d = 7.6 \text{ m}$ and the longitudinal distances $X_1 = 0, X_1 = 20$, Eqs. (22) and (27) yield, $l_1 = 11 \text{ m}$. Inserting $d = 7.6, X = 0$ and $l_1 = 11$ into Eq. (22) one arrives at $F_a(0, 11) = 0.834$. Finally, with the average value of $L_{\text{AE}}^{(a)}(0) = 65.6 \text{ dB}$, Eq. (26) gives $L_s = 86.2 \text{ dB}$.

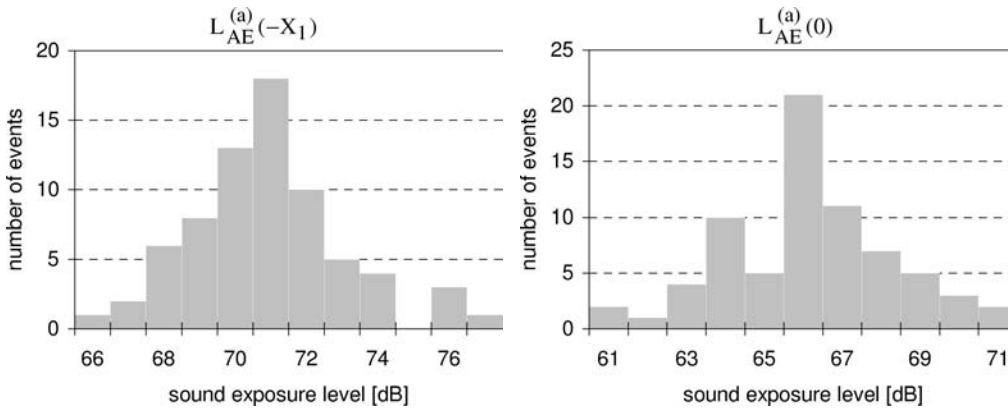


Fig. 8. Histograms of the sound exposure levels of the approach noise, $L_{\text{AE}}^{(a)}(-X_1)$ and $L_{\text{AE}}^{(a)}(0, d)$.

4.2. Bump noise

The bump noise is emitted when a vehicle moves over the bump $(-\varepsilon < x < +\varepsilon)$. It is assumed that the bump is so narrow $(\varepsilon \rightarrow 0)$ that the Dirac delta function, $\delta(x)$,

can be applied. The sound exposure of the bump is (Eqs. (2), (5), (13)),

$$E_b = \frac{\rho c}{4\pi} \int_{-\varepsilon}^{+\varepsilon} \frac{S_b(x) dx}{(x - X)^2 + d^2} \tag{28}$$

where $\varepsilon \rightarrow 0$ and Eqs. (9), (10), (17), (24), (28) imply,

$$L_{AE}^{(b)} = L_s + 10 \log \left\{ \frac{d_0 l_b}{4\pi[X^2 + d^2]} \right\} \tag{29}$$

If the sound exposure level of the bump noise, $L_{AE}^{(b)}$, and the location of microphone (X, d) are known, then the bump noise coefficient can be calculated from (Eq. (29)),

$$l_b = 4\pi \frac{X^2 + d^2}{d_0} 10^{0.1[L_{AE}^{(b)} - L_s]} \tag{30}$$

Example 2

The results of 71 measurements of bump noise (generated by the same vehicles as in Example 1) are shown in Fig. 9, with the average value of $L_{AE}^{(b)} = 63.2$ dB. The microphone was located opposite to the centre of the bump. With the longitudinal distances $X = 0$ and the perpendicular distance $d = 7.6$ m (Fig. 10), Eq. (30) yields the bump noise coefficient, $l_b = 3.6$ m.

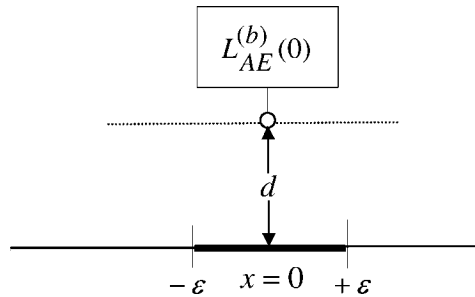
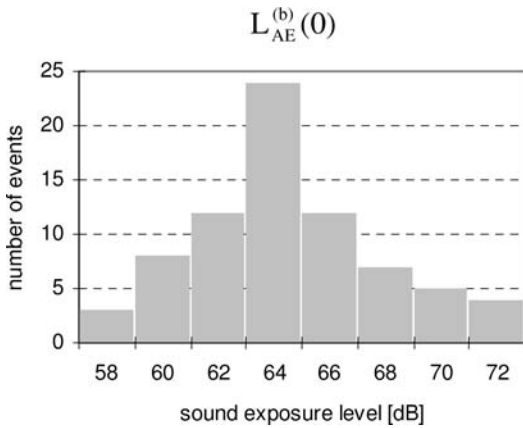


Fig. 9. Histogram of the sound exposure level of the bump noise, $L_{AE}^{(b)}(0)$.

Fig. 10. Microphone location at the bump noise measurement.

4.3. Departure noise

Departure noise is produced when the vehicle moves away from the bump, $x = +\varepsilon$, to $x = +\infty$ (Fig. 5). It is composed of the acceleration noise ($+\varepsilon, +l_2$) with $\varepsilon \rightarrow 0$, and

cruise noise $(+l_2, +\infty)$ (Fig. 6). For the microphone M at the longitudinal distance X from the bump, the corresponding sound exposure level $L_{\text{AE}}^{(d)}(X, l_2)$ can be calculated from Eq. (16), with the sound exposure of the departure noise,

$$E_d(X, l_2) = E_2(+\varepsilon, +l_2) + E_{c2}(+l_2, +\infty), \quad (31)$$

with $\varepsilon \rightarrow 0$. The sound exposure of the deceleration noise can be calculated from Eqs. (2), (5),

$$E_2 = \frac{\rho c}{4\pi} \int_{+\varepsilon}^{+l_2} \frac{S_2(x) dx}{(x - X)^2 + d^2}, \quad (32)$$

where the linear density of sound energy, $S_2(x)$, is defined by Eq. (11). The sound exposure of cruise noise equals (Eqs. (2), (5), (7)),

$$E_{c2} = \frac{\rho c}{4\pi} S_c \int_{+l_2}^{+\infty} \frac{dx}{(x - X)^2 + d^2}. \quad (33)$$

Finally, Eqs. (9), (31)–(33) yield the sound exposure of the departure noise,

$$E_d = \frac{\rho c S_c}{4\pi d} F_d(X, l_2), \quad (34)$$

where

$$F_d(X, l_2) = \frac{d}{2l_2} \ln \left(\frac{(l_2 - X)^2 + d^2}{X^2 + d^2} \right) + \frac{X}{l_2} \left[\tan^{-1} \left(\frac{l_2 - X}{d} \right) + \tan^{-1} \left(\frac{X}{d} \right) \right] + \frac{\pi}{2} - \tan^{-1} \left(\frac{l_2 - X}{d} \right). \quad (35)$$

Making use of Eqs. (17) and (34) one arrives at the sound exposure level of the departure noise,

$$L_{\text{AE}}^{(d)}(X) = L_s + 10 \log \left\{ \frac{d_0}{4\pi d} F_d(X, l_2) \right\}, \quad (36)$$

where L_s (Eq. (24)) could be calculated from the measurements of the approach noise (see Example 1).

To determine the acoustical length of departure l_2 , one measurement of the sound exposure level $L_{\text{AE}}^{(d)}$ has to be made at $X = 0$ (opposite to the bump centre). Then Eq. (36) yields:

$$F_d(0, l_2) = \frac{4\pi d}{d_0} 10^{0.1[L_{\text{AE}}^{(d)}(0) - L_s]}, \quad (37)$$

where the explicit form of the function $F_d(0, l_2)$ is defined by Eq. (35).

Example 3

The microphone was located opposite to the centre of the bump, i.e. at position: $X = 0$, $d = 7.6$ m (Fig. 11). The results of 71 measurements of $L_{AE}^{(d)}(0)$ are shown in Fig. 12. The average value is: $L_{AE}^{(d)}(0) = 66.3$ dB. With the perpendicular distance $d = 7.6$ m and the longitudinal distance $X = 0$, Eqs. (35), (37) give $l_2 = 11.5$ m.

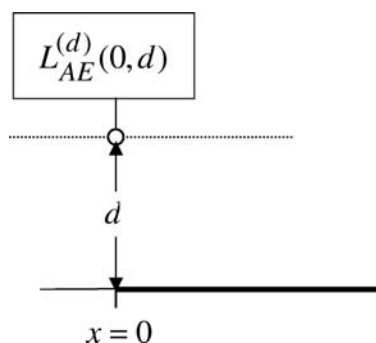


Fig. 11. Microphone location at the departure noise measurement.

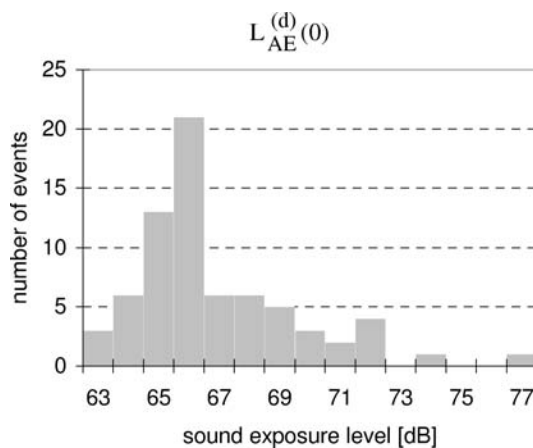


Fig. 12. Histogram of the sound exposure levels of the departure noise $L_{AE}^{(d)}(0)$.

5. Conclusions

To calculate the efficiency of noise reduction due to a road bump η (Eq. (16)), the acoustical lengths of deceleration and acceleration (l_1 , l_2), as well as, the bump noise coefficient (l_b) are needed. All three parameters are available from L_{AE} measurements in an open space, without reflecting objects nearby, when the shortest distance from line of vehicle motion and the microphone, d , is a few meters.

For the case under consideration, the 71 measurements of vehicle noise yield: $l_1 = 11.0$ m (Example 1), $l_b = 3.6$ m (Example 2), and $l_2 = 11.5$ m (Example 3). Substitution of all of them into Eq. (16) gives the road bump noise efficiency: $\eta \approx 0.58$.

Acknowledgments

This work was financially supported by the Environmental Protection Department of Poznań City Hall, headed by Mr. L. Kurek. The authors are grateful to Miss K. Bondar, K. Jarosz, K. Ostrowska, and Mr. W. Deutschman for technical assistance.

References

- [1] KOKOWSKI P., MAKAREWICZ R., *Predicted effects of a speed bump on light vehicle noise*, Applied Acoustics, **67**, 570–579 (2006).
- [2] BOVY P., *Carres berlinois et rigoles, evaluation et recommandation d'aménagement*, Securite dans les rues de quartier in EPFL, Lausanne, Report IREC 1007, 1993.
- [3] Traffic Advisory Leaflets, Speed Cushions, TRL, Crowthorne, Report 4/94, 1994.
- [4] ABBOTT P., TYLER J., LAYFIELD R., *Traffic calming – vehicle noise emissions along side speed control cushions humps*, TRL, Crowthorne, Report 180, 1995.
- [5] Traffic Advisory Leaflets: 75 mm High Road Humps, TRL, Crowthorne, Report 2/96, 1996.
- [6] MIKAMI T., OSHINO Y., TACHIBANA H., *Relationship between running speed and sound power levels on urban noise*, Proceedings of Inter-Noise 1998, Christchurch, 1998.
- [7] LELONG J., MICHELET R., *Effect of acceleration on vehicle noise emission*, Proceedings of the Joint Meeting of ASA and DAGA, Berlin 1999.
- [8] BENDSEN H., LARSON L., *Stoj ved bump pa veje*, Danmarks Transport Forskning, Report 2, Copenhagen 2001.
- [9] LECLERQ L., LELONG J., *Dynamic valuation of urban noise*, Proceedings of ICA 2001, Roma 2001.
- [10] DESARNAULDS V., MONAY G., CALVARO A., *Noise reduction by urban traffic management*, Proceedings of ICA 2001, Kyoto 2004.
- [11] EJSMONT J. A., RONOWSKI G., *Vehicle and tyre/road noise during interrupted-flow traffic conditions*, Proceedings of Inter-Noise 2005, Rio de Janeiro 2005.
- [12] PICAUT J., BERENGIER M., ROUSSEAU E., *Noise impact modeling of a roundabout*, Proceedings of Inter-Noise 2005, Rio de Janeiro 2005.
- [13] EMBLETON T. F. W., *Tutorial on sound propagation outdoors*, Journal of the Acoustical Society of America, **100**, 31–48 (1996).
- [14] KOKOWSKI P., MAKAREWICZ R., *Interrupted traffic noise*, Journal of the Acoustical Society of America, **101**, 360–371 (1997).
- [15] MAKAREWICZ R., FUJIMOTO M., KOKOWSKI P., *A model of interrupted road traffic noise*, Applied Acoustics, **57**, 129–137 (1999).
- [16] MAKAREWICZ R., *Noise from a road intersection*, Acta Acustica with Acustica, **89**, 844–847 (2003).
- [17] PIERCE A. D., *Acoustics*, Acoustical Society of America, New York 1989.